Discovery of Salermide-Related Sirtuin Inhibitors: Binding Mode Studies and Antiproliferative Effects in Cancer Cells Including Cancer Stem Cells

ARTICLE *in* JOURNAL OF MEDICINAL CHEMISTRY · NOVEMBER 2012

Impact Factor: 5.45 · DOI: 10.1021/jm3011614 · Source: PubMed

Journal of Medicinal Chemistry

Article

pubs.acs.org/jmc

Discovery of Salermide-Related Sirtuin Inhibitors: Binding Mode Studies and Antiproliferative Effects in Cancer Cells Including Cancer Stem Cells

Dante Rotili,[†] Domenico Tarantino,[†] Angela Nebbioso,[‡] Chantal Paolini,[§] Covadonga Huidobro,[∥] Ester Lara,[⊥] Paolo Mellini,[†,#] Alessia Lenoci,[†] Riccardo Pezzi,[†] Giorgia Botta,[†] Maija Lahtela-Kakkonen,[#] Antti Poso,[#] Christian Steinkühler,[§] Paola Gallinari,[§] Ruggero De Maria,[▽] Mario Fraga,[∥,⊥] Manel Esteller,[○,◆,¶] Lucia Altucci,[‡,+] and Antonello Mai*[,†]

[†]Istituto Pasteur—Fondazione Cenci Bolognetti, Dipartimento di Chimica e Tecnologie del Farmaco, Università degli Studi di Roma "La Sapienza", P.le A. Moro 5, 00185 Roma, Italy

[‡]Dipartimento di Patologia Generale, Seconda Università degli Studi di Napoli, vico L. De Crecchio 7, 80138 Napoli, Italy

[§]Exiris s.r.l., via Castelfidardo 8, Rome, Italy

[∥]Cancer Epigenetics Laboratory, Instituto Universitario de Oncología del Principado de Asturias (IUOPA), HUCA, Universidad de Oviedo, Oviedo, Spain

[⊥]Department of Immunology and Oncology, National Centre for Biotechnology (CNB-CSIC), Cantoblanco, Madrid, Spain

[#]School of Pharmacy (Pharmaceutical Chemistry), University of Eastern Finland, Kuopio Campus, P.O. Box 1627, 70211 Kuopio, Finland

[▽]Regina Elena National Cancer Institute, Via Elio Chianesi 53, 00144 Rome, Italy

[○]Cancer Epigenetics and Biology Program (PEBC), Bellvitge Biomedical Research Institute (IDIBELL), 08908 L'Hospitalet, Barcelona, Catalonia, Spain

[◆]Department of Physiological Sciences II, School of Medicine, University of Barcelona, Barcelona, Catalonia, Spain

[¶]Institució Catalana de Recerca i Estudis Avançats (ICREA), Barcelona, Catalonia, Spain

[+]CNR-IGB, Institute of Genetics and Biophysics, via P. Castellino, 80100, Napoli, Italy

Supporting Information

ABSTRACT: Chemical changes performed on **1a** (sirtinol) led to a series of SIRT1/2 inhibitors, in some cases more potent than **1a** mainly against SIRT1. Tested in human leukemia U937 cells, the benzamide and anilide derivatives **1b**, **1c**, **2b**, and **2c** as well as the 4-(2-phenylpropyl)thioanalogue **4c** showed huge apoptosis induction, while some sulfinyl and sulfonyl derivatives (**5b**, **5c**, and **6a**−**c**) were highly efficient in granulocytic differentiation. When assayed in human leukemia MOLT4 as well as in human breast MDA-MB-231 and colon RKO cancer cell lines, the anilide **2b** (salermide) and the phenylpropylthio analogue **4b** emerged as the most potent antiproliferative agents. Tested on colorectal carcinoma and glioblastoma multiforme cancer stem cells (CSCs) from patients, **2b** was particularly potent against colorectal carcinoma CSCs, while **4b**, **6a**, and the SIRT2-selective inhibitor AGK-2 showed the highest effect against glioblastoma multiforme CSCs. Such compounds will be further explored for their broad-spectrum anticancer properties.

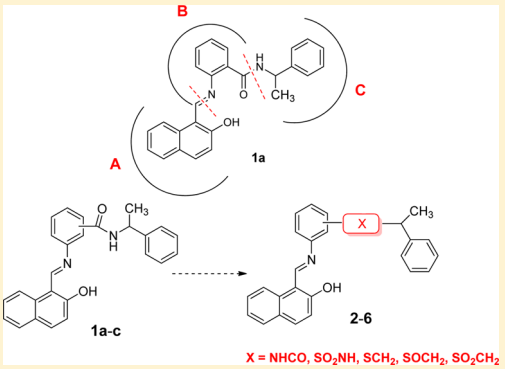

INTRODUCTION

Reversible protein acetylation is an important posttranslational modification that regulates the function of histones and nonhistone proteins and, by this way, the gene expression at epigenetic level.[1−3] Acetylation of lysine residues, carried out by histone/protein acetyltransferases (HATs), is counteracted by the activity of histone/protein deacetylases (HDACs), which remove acetyl groups from the same targets.[4,5]

Among deacetylases, sirtuins (class III HDACs, SIRT1−7) use NAD^+ as cosubstrate for their unique deacetylation chemistry, show no homology with the other classes of HDACs, and are sensitive to specific inhibitors.[6,7] Besides histones, sirtuins deacetylate and/or ADP-ribosylate many other proteins (transcription factors, enzymes, nuclear

Received: August 7, 2012

   dx.doi.org/10.1021/jm3011614 | J. Med. Chem. XXXX, XXX, XXX−XXX

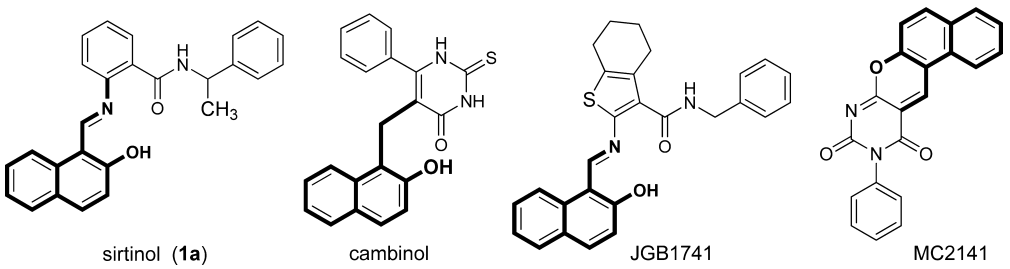

Figure 1. Known SIRT1/2 inhibitors sharing the 2-hydroxy-1-naphthyl pharmacophore moiety.

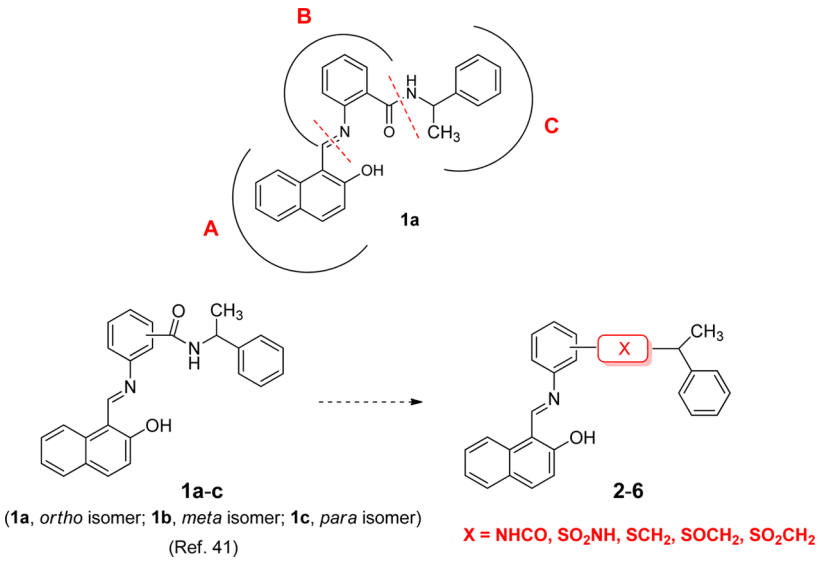

Figure 2. Strategy for the design of novel (2-hydroxy-1-naphthylmethylene)aminophenyl derivatives related to **1a**.

receptors, and other regulatory and structural proteins) and play a critical role in regulation of a variety of cell processes, from apoptosis to control of energetic metabolism and aging.[8−12]

In cancer, the role of sirtuins is actually highly debated. In particular, SIRT1 has been reported as either tumor promoter or tumor suppressor protein.[13,14] In fact, it was found overexpressed in some malignancies (melanoma, prostate, liver, breast, colorectal, and ovarian epithelial cancer)[15−19] and reduced in others (glioblastoma, bladder, colon, ovary, and prostate cancer).[20−24] SIRT1 is also able to inactivate at transcriptional and posttranslational level some tumor suppressor proteins (p53, p73, etc.) and to activate the oncoprotein BCL6, to exert antiapoptotic and antidifferentiation activities through deacetylation of specific transcription factors (E2F1, FOXO3a, Ku70, etc.), and to regulate DNA repair, cell cycle progression, and chromosomal stability.[25] On the other hand, in $APC^{-/+}$ mice transgenic expression of SIRT1 reduced polyp formation, a potential precursor to colorectal cancer[26] (however, $APC^{-/+}$/SIRT null mice did not show increased number of polyps),[27] and $SIRT1^{+/-}/p53^{+/-}$ mice were reported to develop tumors in multiple organs.[24] Altogether, these and other findings suggest that SIRT1 could play different roles in tumorigenesis according to the specific tissue and/or context of tumor.[13,14,25] SIRT2 was previously considered less involved in cancer development than SIRT1 due to its predominantly cytosolic localization and its ability to deacetylate α-tubulin in addition to histones. Nevertheless, recent reports highlighted the role of SIRT2 in the pathogenesis and development of cancer,[28−30] and targeting both SIRT1 and −2 has been suggested as the best therapeutic option.[31]

Among the SIRT1/2 inhibitors described so far, only nicotinamide,[32] sirtinol (**1a**),[33] cambinol,[34] JGB1741,[35] and the benzodeazaoxaflavin (BDF4) MC2141,[36] the last four all sharing the same 2-hydroxy-1-naphthyl pharmacophore moiety (Figure 1), and the structurally different tenovins[37] were found active as antiproliferative agents, alone or in combination with other chemotherapeutics, in a variety of cancer cells.[38−40]

Compound **1a** (2-[(2-hydroxy-1-naphthylmethylene)-amino]-*N*-(1-phenylethyl)benzamide) is a very attractive molecule because its structure can be dissected into three fragments (A, 2-hydroxy-1-naphthylmethylene; B, 2-iminobenzamide; C, *N*-1-phenethylamino) that can individually be manipulated to obtain novel analogues with potential improved activity (Figure 2). The cited JGB1741,[35] with the replacement of the anthranilic moiety of **1a** with the 2-amino-4,5,6,7-tetrahydrobenzo[*b*]thiophene-3-carboxylic acid (Figure 1), offers an example of a successful fragment B modification.

In 2005, we reported some **1a** analogues with changes at the B or C fragments.[41] Among them, only compounds bearing the *N*-(1-phenylethyl)amino side chain shifted from *ortho*- to *meta*- (**1b**) or *para*- (**1c**) position of the benzene ring (Figure 2) showed improved activity against SIRT1 and SIRT2.[41] In yeast phenotypic screening, **1b** and **1c** were as potent as **1a**.[41] No data on their effects on human cells were reported.

Pursuing our researches on sirtuin modulators,[36,42−46] we designed a number of **1a**-related derivatives by replacing the benzoyl amide linkage of the prototype with other bioisosteric groups such as retroamide, sulfonamide, thiomethyl, sulfinyl-

dx.doi.org/10.1021/jm3011614 | J. Med. Chem. XXXX, XXX, XXX−XXX

Scheme 1[a]

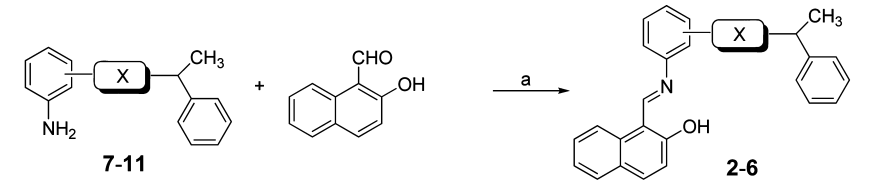

X = **7a**: 2-NHCO; **7b**: 3-NHCO; **7c**: 4-NHCO;
8a: 2-SO_2NH; **8b**: 3-SO_2NH; **8c**: 4-SO_2NH;
9a: 2-SCH_2; **9b**: 3-SCH_2; **9c**: 4-SCH_2;
10a: 2-$SOCH_2$; **10b**: 3-$SOCH_2$; **10c**: 4-$SOCH_2$;
11a: 2-SO_2CH_2; **11b**: 3-SO_2CH_2; **11c**: 4-SO_2CH_2

X = **2a**: 2-NHCO; **2b**: 3-NHCO; **2c**: 4-NHCO;
3a: 2-SO_2NH; **3b**: 3-SO_2NH; **3c**: 4-SO_2NH;
4a: 2-SCH_2; **4b**: 3-SCH_2; **4c**: 4-SCH_2;
5a: 2-$SOCH_2$; **5b**: 3-$SOCH_2$; **5c**: 4-$SOCH_2$;
6a: 2-SO_2CH_2; **6b**: 3-SO_2CH_2; **6c**: 4-SO_2CH_2

[a]Reagents and conditions: (a) glacial acetic acid, dry ethanol/benzene 3/1, reflux.

Scheme 2[a]

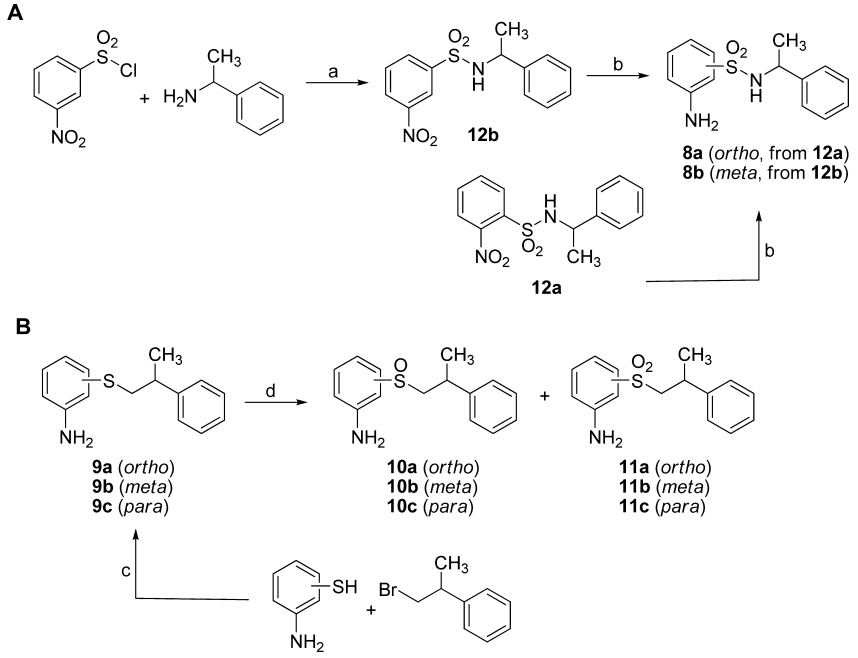

[a]Reagents and conditions: (a) triethylamine, dry dichloromethane, room temperature; (b) stannous chloride dihydrate, 35% HCl, ethanol, room temperature; (c) potassium carbonate, dry DMF, room temp; (d) 30% hydrogen peroxide (w/w), sodium tungstate dihydrate, glacial acetic acid/water, 65 °C.

methyl, and sulfonylmethyl and bearing the 1-phenylethyl side chain with *ortho*, *meta*, or *para* regiochemistry (Figure 2). The compounds **2**–**6** were tested in vitro against human recombinant (hr) SIRT1 and SIRT2, and in human myeloid leukemia U937 cells, together with **1a**–**c**, to evaluate their effects on cell cycle, apoptosis induction, and differentiation. From this preliminary screening, salermide (**2b**)[46] and some analogues were chosen for further experiments.[46] Among the tested cancer cell lines, the leukemia MOLT4 cell line was the most sensitive to the antiproliferative action of **2b** and related derivatives.

Cancer stem cells (CSCs) have been described in many solid and hematologic malignancies as a subset of highly tumorigenic cells with distinct properties such as self-renewal, activation of pluripotency genes, and multidrug resistance. CSCs were shown to resist to conventional cancer therapies, and are reputed to play a major role in cancer relapse.[47,48] Thus, **2b** and selected analogues were tested against two colorectal carcinoma (CRO and 1.1) and two glioblastoma (30P and 30PT) CSCs from patients to determine their potential antiproliferative effects.

CHEMISTRY

The (2-hydroxy-1-naphthylmethylene)amino-*N*-phenylderivatives **2**–**6** were obtained by final condensation between 2-hydroxy-1-naphthaldehyde and the appropriate aniline derivatives **7**–**11** in acidic medium (Scheme 1).The *N*-(2-, 3-, and 4-aminophenyl)-2-phenylpropanamides **7a**–**c** were prepared according to literature by reaction of (*R*/*S*)-2-phenylpropionic acid with the proper phenylendiamine in the presence of BOP reagent or similar.[46,49−51] Commercially available 2-, 3-, and 4-nitrobenzenesulfonyl chlorides treated with (*R*/*S*)-1-phenylethylamine under standard conditions led to the 2-, 3-, and 4-nitro-*N*-(1-phenylethyl)benzenesulfonamides **12a**–**c**, which were in turn reduced to the corresponding 2-, 3-, and 4-amino-*N*-(1-phenylethyl)benzenesulfonamides **8a**–**c** using stannous chloride dihydrate in acidic medium. (See Scheme 2A for the synthesis of the unknown 3-nitro-*N*-(1-phenylethyl)-benzenesulfonamide **12b** and of the 2- and 3-amino analogues

dx.doi.org/10.1021/jm3011614 | J. Med. Chem. XXXX, XXX, XXX−XXX

8a,**b**. The 2- and 4-nitro derivatives as well as the 4-amino-*N*-(1-phenylethyl)-benzenesulfonamide **8c** are known.)[43,52] The 2-, 3-, and 4-(2-phenylpropylthio)anilines **9a**−**c** were prepared by alkylation under basic conditions of the proper aminothiophenols with 1-bromo-2-phenylpropane.[43] Further oxidation of **9a**−**c** with sodium tungstate dihydrate afforded a mixture of the corresponding 2-, 3-, and 4-(2-phenylpropylsulfinyl)anilines **10a**−**c** and 2-, 3-, 4-(2-phenylpropylsulfonyl)anilines **11a**−**c**, which were separated by column chromatography, recrystallized, and used in the subsequent condensation with 2-hydroxy-1-naphthaldehyde (Scheme 2B).

Chemical and physical data of compounds **2**−**6** are listed in Table S1 in Supporting Information. Chemical and physical data of the intermediate compounds **8a**, **8b**, **9a**−**c**, **10a**−**c**, **11a**−**c**, and **12b** are listed in Table S2 in Supporting Information.

RESULTS AND DISCUSSION

SIRT1 and SIRT2 Assays. The (2-hydroxy-1-naphthylmethylene)amino-*N*-phenyl derivatives **2**−**6** were tested in vitro against SIRT1 and SIRT2 using a fluorogenic substrate and NAD^+.[44] The IC_{50} (inhibitory concentration 50, compound dose required to inhibit the enzyme activity of 50%) values of **2**−**6** are graphed in Figure 3. IC_{50} values of **1a**, **1b**, and **1c** against SIRT1 and SIRT2 were added for comparison.

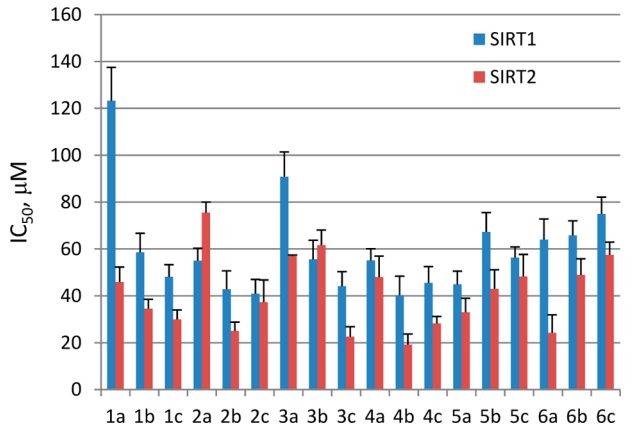

Figure 3. IC_{50} values of **1**−**6** against SIRT1 and SIRT2.

Against SIRT1, compounds **2**−**6** showed quite similar inhibiting activity, with IC_{50} values ranging from 40.3 to 67.3 μM regardless of the nature or regiochemistry of the side chain. The only exceptions were **3a** and **6c**, which displayed lower potency, whereas the 4-phenylpropionamide derivative **2c** and the (2-phenylpropyl)thio derivative **4b** were the most efficient inhibitors, with IC_{50} values of 40.9 and 40.3 μM, respectively. In comparison with the reference compounds, the majority of **2**−**6** derivatives displayed inhibition potencies higher than **1a** and similar to **1b** and **1c**.

In general terms, in anti-SIRT2 assay the tested compounds **2**−**6** exhibited similar or higher inhibiting activities than against SIRT1, albeit with some exceptions (**2a** and **3b**). Among compounds substituted with 2-phenylpropionamide function, the *meta* analogue **2b** (salermide) displayed the highest activity (IC_{50} = 25.0 μM), while in the **3** series the 4-*N*-(1-phenylethyl)benzenesulphonamide **3c** was the most efficient (IC_{50} = 22.6 μM). In the (2-phenylpropyl)thio-substituted series, the highest SIRT2 inhibiting activity was shown by the *meta* (**4b**) and the *para* (**4c**) analogues, **4b** being the most potent (IC_{50} = 19.2 μM) among all the tested derivatives. Similar potency against SIRT2 was also observed with the 2-(2-phenylpropyl)sulfonyl derivative **6a** (IC_{50} = 24.2 μM).

Docking Studies. The structural variability of the compounds with *ortho*, *meta*, and *para* substituents offers the possibility of different interaction modalities in the binding site that could result in some cases in a differential activity on SIRT1 and SIRT2. To study the effect of the substitution of the (2-hydroxy-1-naphthylmethylene)amino-*N*-phenyl derivatives **2**−**6** on the binding in the NAD^+ pocket, **2**−**6** were docked into SIRT1 and SIRT2. Our docking studies showed that there were little differences in docking poses for most of the compounds. In contrast, in the case of compound **1a**, the β-naphthol ring is completely out of SIRT1 binding site (Figure 4A), while for SIRT2 (Figure 4B) the **1a** β-naphthol ring is placed in the B-pocket (the ribose moiety binding pocket of NAD^+, in blue in Figure 4) and the phenyl ring is oriented toward the C-pocket (a nicotinamide binding site, in yellow in Figure 4). Compound **1a** forms two hydrogen bonds with Thr262 and Ser98 of SIRT2, increasing the affinity of binding compared to SIRT1. Differently from **1a**, **4b**, the most efficient inhibitor reported in this study, has the β-naphthol ring placed in the B-pocket in both SIRT1 (Figure 4C) and SIRT2 (Figure 4D).

Nevertheless, in SIRT1, **4b** does not have a perfect fit in the binding pose because there are different exposed areas. In SIRT2, **4b** is binding from the A to C pocket and shows a correct fit in NAD^+ binding site. This might be due to openness of C-pocket in SIRT2 and to favorable interactions in the C-pocket between Phe96 and His187 established by **4b** in SIRT2 (Figure 4D).

The conclusion from docking studies is that the most potent compounds show a common binding mode for SIRT2: the β-naphthol ring has enough space to fit in B-pocket and the rest of the scaffold can enter into the C-pocket. On the contrary, in the case of SIRT1, there is less space in B-pocket, the scaffold has no optimal fit in it, and the C-pocket is practically empty, so that only suboptimal complementary binding is achieved in SIRT1 (see Supporting Information).

Cell Cycle Effect, Apoptosis Induction, And Granulocytic Differentiation on Human Leukemia U937 Cells. The (2-hydroxy-1-naphthylmethylene)amino-*N*-phenyl derivatives **1**−**6** were tested at 5, 25, and 50 μM in human leukemia U937 cells in order to determine their effects on cell cycle, apoptosis, and granulocytic differentiation. At 5 μM, no effect was detected, and at 50 μM, many compounds showed massive apoptosis (see Figures S11−S12 in Supporting Information). Figure 5 shows cellular data for **1**−**6** tested on U937 cells at 25 μM for 40 h. EX-527,[53] a well-known potent and selective SIRT1 inhibitor typically devoid of effects on cell growth and viability,[54] and AGK-2,[55] a SIRT2-selective inhibitor useful in Parkinson's disease models, were used as reference drugs both at 25 μM.

Under the tested conditions, among the **2** series the 2-(2-phenylpropionamide) derivative **2a** displayed a block at the S phase of cell cycle, whereas the corresponding 3- and 4-isomers **2b** and **2c** gave an evident arrest at the G1 phase, similar to that detected with **1b** and **1c**. Cells treated with the 3-*N*-(1-phenylethyl)sulphonamide compound **3b** showed a clear arrest at the S phase, whereas with the 4-(2-phenylpropylsulfonyl) analogue **6c**, a block of cell cycle at the G1 phase was observed

dx.doi.org/10.1021/jm3011614 | J. Med. Chem. XXXX, XXX, XXX−XXX

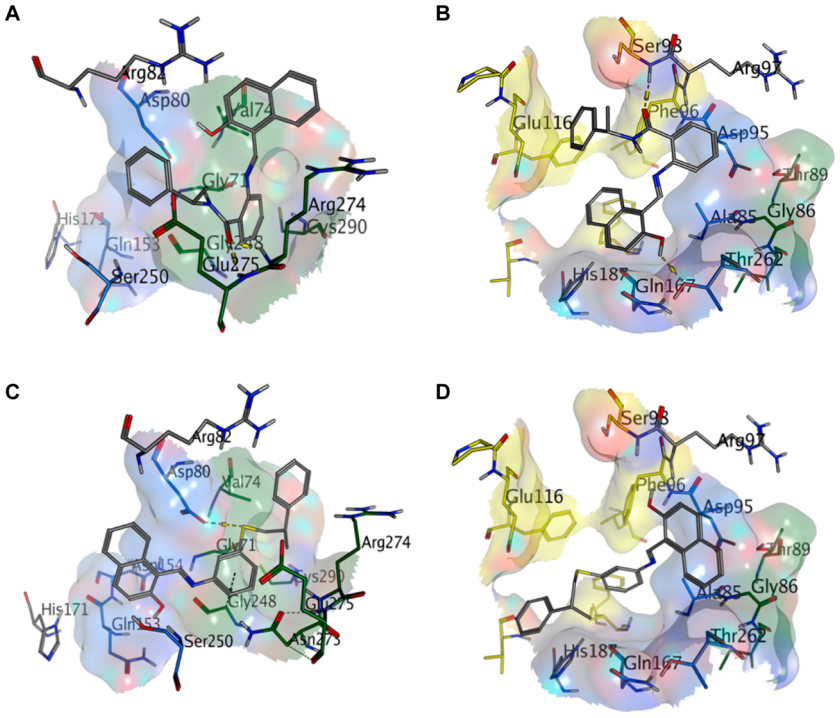

Figure 4. Docking poses for **1a** in SIRT1 (A) and SIRT2 (B), and docking poses for the most potent derivative **4b** in SIRT1 (C) and SIRT2 (D). The B-pocket (the ribose moiety binding pocket of NAD^+) of the enzymes is depicted in blue, and the C-pocket (a nicotinamide binding site) of the enzymes is depicted in yellow.

(Figure 5A). EX-527 and AGK-2 did not show any change in the U937 cell cycle at the tested conditions. Also combination attempts of EX-527 and AGK-2 failed to give cell cycle alteration and/or apoptosis (see Figure S13 in Supporting Information). The evidence that different phases of cell cycle appear blocked by different compounds that share the same targets (SIRT) might both be related to the different effects on SIRT1 versus SIRT2 or be related to the different inhibitory action in living cells of the compounds. Clearly, we can not exclude that also additional targets might be involved.

Most of the tested compounds exhibited a high pre-G1 peak (an index of apoptosis induction) at the FACS analysis. The reference compound **1a** caused an apoptosis induction of 47% and its regioisomers **1b** and **1c**, as well as the corresponding retroamide analogues **2b** and **2c**, led to a percentage of apoptosis near (or over) 70%. In this assay, the 4-(2-phenylpropyl)thio derivative **4c** showed massive apoptosis so that we fixed the cutoff at 90% (Figure 5B). Contrarily, EX-527 and AGK-2, alone or in combination (Figure S13 in Supporting Information), were ineffective in inducing apoptosis.

Granulocytic differentiation was evaluated by counting the number of cells expressing the superficial antigen CD11c and subtracting from this value the number of dead [propidium iodide (PI) positive] cells. Under the tested conditions, mainly the (2-phenylpropyl)sulfinyl (**5b**, **5c**) and the (2-phenylpropyl)sulfonyl (**6a**–**c**) derivatives displayed high percentage of CD11c positive/PI negative cells, with values ranging from 57.3 to 85.6% (Figure 5C). Also, in this test, no effects were detected using EX-527 and AGK-2.

Antiproliferative Effect on Several Cancer Cell Lines. All the described compounds **2**–**6**, including **1b** and **1c** for comparison, were tested first at 25 μM on human leukemia MOLT4 cells for 24, 48, and 72 h to determine their antiproliferative effects (MTT method) (Figure S14 in Supporting Information). In addition, selected compounds bearing the (2-hydroxy-1-naphthylmethylene)amino-*N*-phenyl moiety linked to *N*-(1-phenylethyl)benzamide (**1b**), 2-phenylpropionamide (**2a** and **2b**), *N*-(1-phenylethyl)sulphonamide (**3b**), (2-phenylpropyl)thio (**4a** and **4b**), and (2-phenylpropyl)-sulfonyl (**6a** and **6b**) groups were tested first at 25 μM on human breast cancer MDA-MB-231 and human colon cancer RKO cells (Figure S15 in Supporting Information). At 25 μM, in MOLT4 cells **1c**, **2b**, **4a**, **4b**, **5a**, **5b**, and **6a** were able to arrest to some extent the cell growth. At the same concentration, only **2b** (salermide), among the tested derivatives, showed some antiproliferative effects on MDA-MB-231 and RKO cells and was therefore chosen for further studies.[46]

Selected compounds **2b**, **4a**, **4b**, and **6b** were then tested at 50 μM in MOLT4, MDA-MB-231, and RKO cells for 24, 48, and 72 h, and their antiproliferative effect was determined (Figure 6). In these assays, **2b** and **4b** emerged as the most efficient compounds to hamper the growth of the three tested cancer cell lines. Finally, some compounds (**1c**, **2b**, **2c**, **3a**, **3c**, **4c**, **5a**, **5b**, **5c**, and **6c**) were tested at 100 μM in MOLT4 cells, and at this concentration **1c**, **2b**, **2c**, **5a**, and **5c** displayed high, time-dependent growth arrest (Figure S16 in Supporting Information).

Antiproliferative Activity on Cancer Stem Cells (CSCs): Effect of Selected 2–6 Derivatives on Two Colorectal Carcinoma (CRC) CSC Lines and Two Glioblastoma Multiforme (GBM) CSC Lines. Taking into account the apoptotic, cytodifferentiating, and/or antiproliferative activities displayed in previous assays, we selected compounds **2b**, **4b**, **5a**, **5b**, **6a**, and **6c** to detect their capability to inhibit viability of CSCs, a cancer cell subset highly tumorigenic, resistant to conventional cancer therapies, and believed to play a major role in cancer relapse.[48] The SIRT1-selective inhibitor EX-527 and

dx.doi.org/10.1021/jm3011614 | J. Med. Chem. XXXX, XXX, XXX–XXX

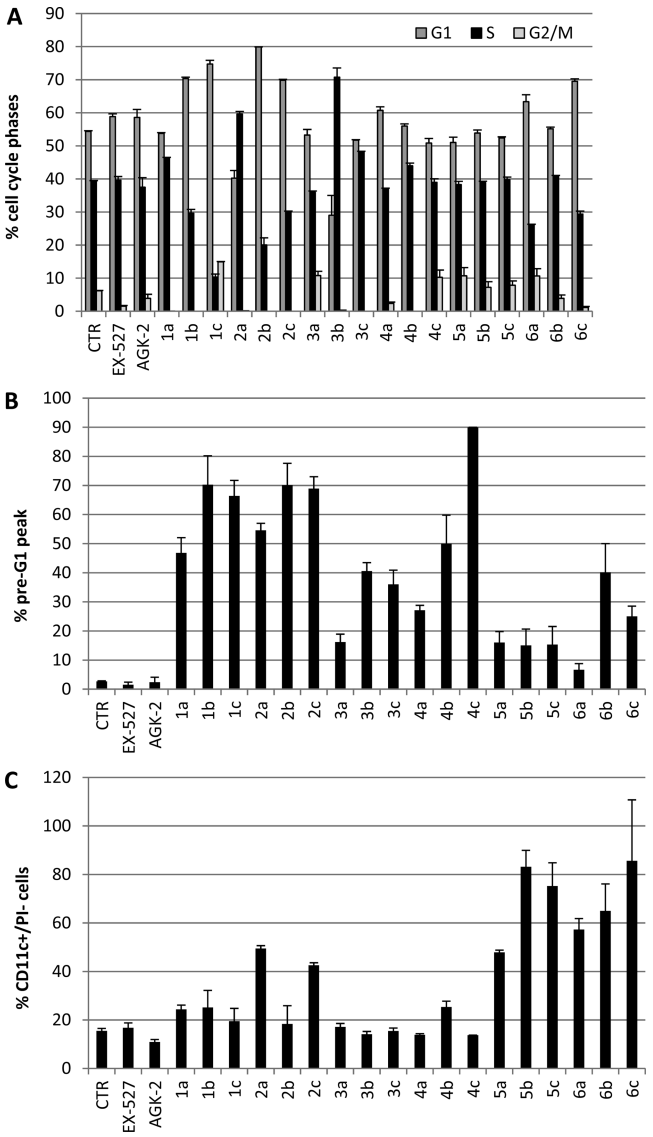

Figure 5. Cell cycle analysis (A), apoptosis induction (B), and granulocytic differentiation (C) obtained treating human leukemia U937 cells with **1**–**6** at 25 μM for 40 h.

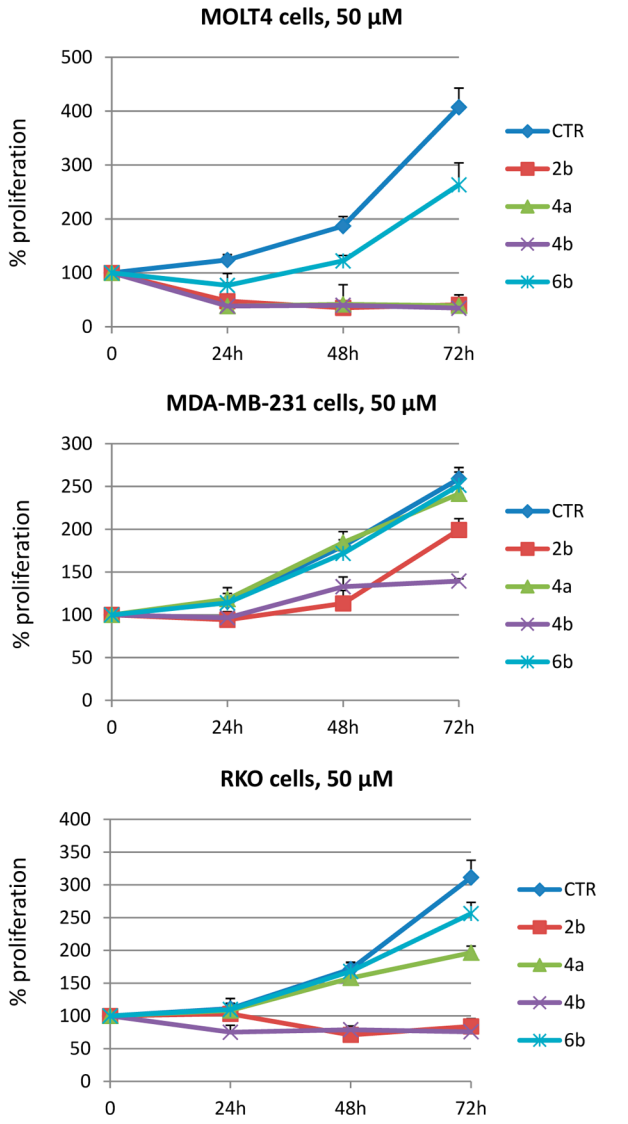

Figure 6. Percentage of antiproliferative activity of **2b**, **4a**, **4b**, and **6b** tested at 50 μM in leukemia MOLT4, breast MDA-MB-231, and colon RKO cancer cells (MTT method).

its SIRT2-selective counterpart AGK-2 were added to the assay. Two colorectal carcinoma (CRC, CRO, and 1.1) and two glioblastoma multiforme (GBM, 30P, and 30PT) CSCs from patients were chosen for this assay. After 72 h of treatment, the CC_{50} (cytotoxic concentration able to kill 50% of the cells) values were determined and are reported in Table 1. The corresponding dose–response curves are reported in Supporting Information Figure S17.

Against the tested CSCs, EX-527 failed to produce significant growth inhibition up to 50 μM, whereas AGK-2 displayed good antiproliferative activity against GBM CSCs in which it was the most potent among the tested derivatives. Compound **2b** (salermide), under the tested conditions, was highly efficient in reducing CRC CSC viability, bearing single-digit μM activity [CC_{50} = 6.7 (CRO) and 9.7 (1.1) μM], while it was much less potent in GBM CSCs (CC_{50} = 41.0 (30P) and 36.5 (30PT) μM).

With respect to **2b**, compounds **4b** and **6a** exhibited lower potency on CRC CSCs, with CC_{50} values ranging from 14.5 to 20 μM, and higher potency on GBM CSCs (CC_{50} = 15.3 to

Table 1. Cell Viability Inhibition by 2b, 4b, 5a, and 6a in CRC and GBM CSCs[a]

	CC_{50}, μM			
	CRC CSCs		GBM CSCs	
compd	CRO	1.1	30P	30PT
2b	6.7 ± 1.2	9.7 ± 3.1	41.0 ± 5.2	36.5 ± 2.5
4b	14.5 ± 1.2	20.0 ± 2.8	15.5 ± 1.9	15.6 ± 3.6
5a	33% inhibition[b]	46% inhibition[b]	42% inhibition[b]	39% inhibition[b]
5b	ND[c]	23.4 ± 0.6	35.0 ± 1.9	ND
6a	15.7 ± 1.0	19.5 ± 0.7	17.4 ± 1.7	15.3 ± 3.1
6c	ND	34.0 ± 2.2	30.2 ± 1.8	ND
EX-527	20% inhibition[b]	no inhibition[b]	10% inhibition[b]	20% inhibition[b]
AGK-2	50% inhibition[b]	50% inhibition[b]	12.5 ± 0.5	9.6 ± 1.0

[a]Values are means of three experiments. [b]At 50 μM. [c]ND, not detected.

dx.doi.org/10.1021/jm3011614 | J. Med. Chem. XXXX, XXX, XXX–XXX

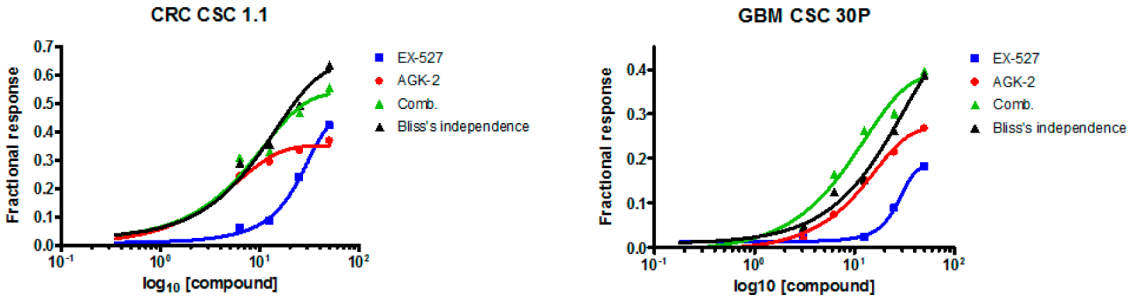

Figure 7. Effects of EX-527 plus AGK-2 combination in CRC 1.1 and GBM 30 P CSCs.

17.4 μM), in this last case being only slightly less efficient than AGK-2. Remaining compounds **5b** and **6c**, chosen because of their high cytodifferentiation effect in U937 cells, displayed low antiproliferative activities against both the tested CSC lines.

Combination assays of EX-527 and AGK-2 were carried out to ascertain the potential benefit derived from dual SIRT1/2 inhibition. The combined cytotoxic effects of EX-527 and AGK-2 on CRC 1.1 and GBM 30P CSC clones are shown in Figure 7. While for the CRC 1.1 clone the experimental combination data conformed to the Bliss's additive model, the two compounds resulted to act synergistically on the GBM 30P clone.

CONCLUSION

Chemical manipulations (replacing the benzamide with an anilide, sulphonamide, thiomethyl, sulfinylmethyl, or sulfonylmethyl moiety and/or shifting the side chain from *ortho* to *meta* or *para* position of the benzene ring) were performed on the **1a** scaffold to obtain (2-hydroxy-1-naphthylmethylene)amino-*N*-phenyl derivatives **2**−**6**, many of which with improved activity against both SIRT1 and SIRT2. The higher inhibitory activity of **4b**, the most potent compound in this series, with respect to the prototype **1a** has been rationalized through docking studies. When tested in U937 human leukemia cells (25 μM, 40 h), the 4-(2-phenylpropyl)thio derivative **4c** displayed massive apoptosis, and the *meta*- and *para*-benzamide and -anilide derivatives **1b**,**c** and **2b**,**c** showed cell cycle arrest at the G1 phase joined to high apoptosis. Differently, the sulfinyl and sulfonyl analogues **5b**,**c** and **6a**−**c** were the most efficient in inducing granulocytic differentiation in U937 cells at the same conditions. Selected **2**−**6** compounds were screened for assessing their antiproliferative activity against human leukemia MOLT4 cell lines, human breast MDA-MB-231, and colon RKO cancer cell lines at 25, 50, and (in some cases) 100 μM for 24, 48, and 72 h. From the overall results, **2b** (salermide) and **4b** emerged as two of the most potent derivatives able to block cell growth in the tested cancer cell lines. Thus, **2b** and **4b** as well as the sulfinyl and sulfonyl derivatives **5a**,**b** and **6a**,**c** were tested against two colorectal carcinoma (CRO and 1.1) and two glioblastoma multiforme (30P and 30PT) CSCs, in comparison with the SIRT1-selective inhibitor EX-527 and the SIRT2-selective inhibitor AGK-2. Against the tested CSCs, **2b** showed the highest antiproliferative activity on colorectal carcinoma CSCs, with single-digit CC_{50} values, while **4b** and **6a** were 2-fold less potent than **2b**. Against glioblastoma multiforme CSCs, **4b**, **6a**, and AGK-2 displayed the highest potency, thus suggesting a positive, additional role of SIRT2 in the viability and proliferation of CSCs. Combination of EX-527 and AGK-2 in CRC 1.1 gave an additive antiproliferative effect, whereas in GBM 30P CSC clones the two compounds acted synergistically.

Because the most efficient compounds in cells showed activity up to single-digit micromolar concentration, while against SIRTs they displayed inhibition in the 20−50 μM range, the involvement of off-target side effects can not be ruled out.[56]

In conclusion, compounds **2b**, **4b**, and **6a** emerged as highly potent small molecules for anticancer treatment, also against CSCs, that are normally refractory to conventional anticancer therapy and are believed to play a role in cancer relapse. Further studies should be addressed to improve pharmacokinetic and drug-like properties of such compounds.

EXPERIMENTAL SECTION

Chemistry. Melting points were determined on a Buchi 530 melting point apparatus and are uncorrected. ^{1}H NMR spectra were recorded at 400 MHz on a Bruker AC 400 spectrometer; chemical shifts are reported in δ (ppm) units relative to the internal reference tetramethylsilane (Me_4Si). All compounds were routinely checked by TLC and ^{1}H NMR. TLC was performed on aluminum-backed silica gel plates (Merck DC, Alufolien Kieselgel 60 F_{254}) with spots visualized by UV light. All solvents were reagent grade and, when necessary, were purified and dried by standard methods. Concentration of solutions after reactions and extractions involved the use of a rotary evaporator operating at reduced pressure of ca. 20 Torr. Organic solutions were dried over anhydrous sodium sulfate. Elemental analysis has been used to determine purity of the described compounds, that is >95%. Analytical results are within ±0.40% of the theoretical values. All chemicals were purchased from Aldrich Chimica, Milan (Italy) or from Lancaster Synthesis GmbH, Milan (Italy) and were of the highest purity.

General Procedure for the Preparation of Derivatives (2−6). Example: *N*-(4-[(2-Hydroxynaphthalen-1-yl)methyleneamino]-phenyl)-2-phenylpropanamide (2c). A mixture of 2-hydroxy-1-naphthaldehyde (0.36 g, 2.1 mmol) and *N*-(4-aminophenyl)-2-phenylpropanamide[51] (0.50 g, 2.1 mmol) in absolute ethanol/benzene (3/1) (30 mL) was heated at reflux for 4 h in the presence of a catalytic amount of glacial acetic acid. After cooling at room temperature, from the mixture reaction a yellow solid separated, which was collected by filtration, washed with chloroform, and purified by crystallization from toluene/ethanol. ^{1}H NMR ($CDCl_3$) δ 1.63 (d, 3H, $CHCH_3$), 3.76 (m, 1H, $CHCH_3$), 6.63 (m, 2H, aromatic rings), 7.07−8.01 (m, 15H, aromatic rings), 9.30 (s, 1H, C*H*=N), 15.58 (s, 1H, O*H*). Anal. C, H, N.

(*R*/*S*)-3-Nitro-*N*-(1-phenylethyl)benzenesulfonamide (12b). 3-Nitrobenzenesulfonyl chloride (1 equiv, 1 g, 4.51 mmol) was dissolved in 20 mL of dichloromethane and then was added dropwise to a mixture of (*R*/*S*)-1-phenylethylamine (1.1 equiv, 0.64 mL, 4.96 mmol) and triethylamine (1.2 equiv, 0.73 mL, 5.41 mmol) in dichloromethane (50 mL) while cooling with water bath. The resulting mixture was stirred at room temperature for 2 h and then was diluted with water (20 mL), and the aqueous solution was extracted with ethyl acetate (3 × 50 mL). The organic layers were collected, washed with 0.2 N hydrochloric acid (3 × 50 mL), 0.2 N sodium hydroxide (3 × 50

dx.doi.org/10.1021/jm3011614 | J. Med. Chem. XXXX, XXX, XXX−XXX

mL), and brine (3 × 50 mL), dried (sodium sulfate), and evaporated under reduced pressure. The solid residue was then purified by crystallization from toluene to furnish the desired derivative **12b**. ^{1}H NMR ($CDCl_3$) δ 1.50 (d, 3H, $CHCH_3$), 4.63 (q, 1H, $CHCH_3$), 5.35 (d, 1H, N*H* exchangeable with D_2O), 7.01−7.10 (m, 5H, phenyl ring), 7.51 (m, 1H, nitrophenyl ring), 7.93 (m, 1H, nitrophenyl ring), 8.23 (m, 1H, nitrophenyl ring), 8.33 (m, 1H, nitrophenyl ring).Anal. C, H, N, S.

General Procedure for the Preparation of (*R*/*S*)-2- and -3-Amino-*N*-(1-phenylethyl)benzenesulfonamides (8a and 8b). Example: (*R*/*S*)-3-Amino-*N*-(1-phenylethyl)-benzenesulfonamide (8b). A solution of **12b** (1 equiv, 0.99 g, 3.23 mmol) in ethanol (9 mL) was slowly added to a solution of stannous chloride dihydrate (3.5 equiv, 2.55 g, 11.31 mmol) and 37% hydrochloric acid (3 mL) while cooling with ice bath. After 30 min, the reaction was allowed to reach room temperature and then stirred for further 2 h. After the completion of the reaction, the solvent was evaporated under reduced pressure and the residue treated with 2N potassium hydroxide (20 mL) and ethyl acetate (3 × 20 mL). Then, the organic phase was dried (sodium sulfate) and evaporated to afford the desired compound **8b**. ^{1}H NMR ($CDCl_3$) δ 1.42 (d, 3H, $CHCH_3$), 3.66 (s, 2H, NH_2 exchangeable with D_2O), 4.46 (q, 1H, $CHCH_3$), 5.15 (s, 1H, N*H* exchangeable with D_2O), 6.78 (m, 1H, benzenesulfonamide ring), 7.05−7.24 (m, 8H, benzenesulfonamide ring and phenyl ring). Anal. C, H, N, S.

General Procedure for the Preparation of (*R*/*S*)-2-, -3-, and -4-(2-Phenylpropylthio)anilines (9a−c). Example: (*R*/*S*)-4-(2-Phenylpropylthio)aniline (9c). (*R*/*S*)-1-Bromo-2-phenylpropane (1.2 equiv, 1.45 mL, 9.58 mmol) was added to a suspension of 4-aminothiophenol (1 equiv, 0.84 mL, 1.0 g, 7.98 mmol) and anhydrous potassium carbonate (2 equiv, 2.2 g, 15.97 mmol) in dry *N*,*N*-dimethylformamide (5 mL), and the mixture was stirred at room temperature for 2 h. Afterward, the reaction mixture was quenched with water (50 mL) and extracted with ethyl acetate (3 × 50 mL). The organic phase was then washed with brine (2 × 30 mL) and dried over sodium sulfate. After evaporation in vacuum, the crude was purified by column chromatography on silica gel eluting with ethyl acetate/chloroform (1/20) to furnish the desired compound **9c** as a pure oil. ^{1}H NMR ($CDCl_3$) δ 1.39 (d, 3H, $CHCH_3$), 2.93 (m, 2H, SCH_2CHCH_3), 3.09 (m, 1H, CH_2CHCH_3), 6.60−7.33 (m, 9H, aromatic rings). Anal. C, H, N, S.

General Procedure for the Preparation of (*R*/*S*)-2-, -3-, and -4-(2-Phenylpropylsulfinyl)anilines (10a−c) and (*R*/*S*)-2-, -3-, and -4-(2-Phenylpropylsulfonyl)anilines (11a−c). Example: (*R*/*S*)-4-(2-Phenylpropylsulfinyl)aniline (10c) and (*R*/*S*)-4-(2-Phenylpropylsulfonyl)aniline (11c). A mixture of sodium tungstate dehydrate (0.001 g, 0.003 mmol), 1 drop of acetic acid, and water (1 mL) was placed in a flask and heated at 65 °C. (*R*/*S*)-4-(2-Phenylpropylthio)aniline (**9c**) (0.50 g, 2.05 mmol) was added, followed by dropwise addition of 30% w/w hydrogen peroxide (0.36 mL), and the mixture was stirred at 65 °C for 1.5 h. After cooling, 5 mL of water and 5 mL of ethyl acetate were added. The layers were separated, and the aqueous phase was extracted with ethyl acetate (3 × 5 mL). The organic phase was washed with brine and dried over sodium sulfate. The solvent was removed under reduced pressure to furnish a mixture of compounds (0.60 g), which was separated by silica gel column chromatography using ethyl acetate/*n*-hexane (1/1) as eluent. Pure compounds **10c** [R_f = 0.2 (ethyl acetate); yield 57%] and **11c** [R_f 0.6 (ethyl acetate); yield 31%] were obtained. **10c**: ^{1}H NMR ($CDCl_3$) δ 1.42−1.50 (d, 3H, $CHCH_3$), 2.84−3.16 (m, 2H, SCH_2CHCH_3), 3.29 (m, 1H, CH_2CHCH_3), 3.99 (s, 2H, NH_2), 6.75 (m, 2H, aromatic rings), 7.21−7.46 (m, 7H, aromatic rings). Anal. C, H, N, S. **11c**: ^{1}H NMR ($CDCl_3$) δ 1.43 (d, 3H, $CHCH_3$), 3.32 (m, 3H, CH_2CHCH_3 and SCH_2CHCH_3), 4.18 (s, 2H, NH_2) 6.63 (m, 2H, aromatic rings), 7.08−7.26 (m, 5H, aromatic rings), 7.57 (m, 2H, aromatic rings). Anal. C, H, N, S.

SIRT1/2 Inhibition Assay. The SIRT activity assay was performed using: for SIRT1, human Sirtuin 1 (GenBank accession no. NM_012238), amino acid 193−741 with *N*-terminal GST tag, MW = 87.2 kDa, expressed in *Escherichia coli* expression system. For SIRT2: human Sirtuin 2 (hSir2SIRT2) (GenBank accession no. NM_012237), full length, MW = 43 kDa, expressed in *E. coli*. Compounds were tested using a modified Fluor de Lys fluorescence-based assay kit (AK-555, AK-556 Biomol). The assay procedure has two steps: in the first part the SIRT1/2 substrate (50 μg), an acetylated Lys side chain comprising amino acids 379−382 (Arg-His-Lys-Lys(Ac)) (for SIRT1 assay), or 317−320 (Gln-Pro-Lys-Lys(Ac)) (for SIRT2 assay) of human p53 conjugated with aminomethylcoumarin was deacetylated during incubation at 37 °C for 1 h by SIRT1 or SIRT2 in the presence of NAD^+ (500 μg) and the tested compounds (reaction buffer: 50 mM Tris-HCl, pH 8.0, 137 mM NaCl, 2.7 mM KCl, 1 mM $MgCl_2$; add fresh 1 mg/mL BSA, 1% DMSO). The second stage was initiated by the addition of the Developer II, including 2 mM nicotinamide (NAM), a sirtuin inhibitor that stops the SIRT1/2 activity, and the fluorescent signal is produced. The fluorescence was measured on a fluorometric reader (Inphinite 200 TECAN) with excitation set at 360 nm and emission detection set at 460 nm. Counter assay was performed without enzyme: 1 μM standard (fluorogenic unacetylated peptide) + compounds added as above and then developed and fluorescence measured as above. The fluorescence from compounds was subtracted from all signals if there was. Experiments on the SIRT1 and -2 inhibition have been performed in triplicate. IC_{50} data were analyzed using GraphPad Prism Software.

Molecular Modeling. No crystal structure is available for SIRT1, and for SIRT2 there is only apo structure available. Therefore, we were forced to build also homology model for SIRT2 in bioactive conformation. The template used for the homology model of SIRT1 and SIRT2 was the crystal structure of Sir2 homologue from *Archeaoglobus fulgidus* (Sir2-Af1) with NAD^+ (PDB code: 1ici). The homology models of SIRT1 and SIRT2 were built using FUGUE and ORCHESTRA in SYBYL 1.3 (Alignments are presented in Supporting Information).[48] The side chains were optimized by geometry optimization with Amber99 using Molecular Operating Environment (MOE) 2010.10.[49] The ligand structures were built with MOE software and minimized using MMFF94 force field until a rmsd gradient of 0.05 kcal mol^{-1} $Å^{-1}$ was reached. The docking simulations were performed in the NAD^+ binding site of the homology models SIRT1 and -2 using MOE. Default values were used for all docking settings. The best-ranked poses of each docked ligand was included in the analysis. The docking results were visually inspected.

Cell Cycle and Apoptosis Analysis on Human Leukemia U937 Cells. Cells were collected and suspended in 500 μL of hypotonic buffer [0.1% Triton X-100, 0.1% sodium citrate, 50 μg/mL propidium iodide (PI)]. Then the cells were incubated in the dark for 30 min. Samples were acquired on a FACS-Calibur flow cytometer using the Cell Quest software (Becton Dickinson). Analyses were performed with standard procedures using ModFit LT version3 software (Verity). All experiments were performed in triplicate.

Granulocytic Differentiation on U937 Cells. Cells were suspended in 10 μL of phycoerythrine-conjugated CD11c (CD11c-PE). Control samples were incubated with 10 μL of PE conjugated mouse IgG1. The incubations were performed at 4 °C in the dark for 30 min, and after, cells were collected, washed in phosphate buffered saline (PBS), and suspended in 500 μL of PBS containing propidium iodide (PI) (0.25 μg/mL). Samples were analyzed by FACS with Cell Quest technology (Becton Dickinson). PI positive cells have been excluded from the analysis.

Antiproliferative Activity on Human Leukemia MOLT4, Human Breast Cancer MDA-MB-231, and Human Colon Cancer RKO Cell Lines. Cell lines were obtained from the American Type Culture Collection (VA, USA). Cell viability was determined using the 3-(4,5-dimethylthiazol-2-yl)-2,5-diphenyltetrazolium bromide assay as described earlier.[46]

Cell Viability Inhibition in Cancer Stem Cells (CSCs). CSC cultures were established and propagated under spherogenic conditions as described.[57,58] Cells were grown for 20−30 days in CSC serum-free medium containing epidermal growth factor (EGF) and basic fibroblast growth factor (bFGF) and maintained at a concentration of 50000−200000 cells/mL. Medium was replaced every three−five days with fresh medium complemented with 25% conditioned medium, depending on the growth rate and viability of

each cell line. For the cell viability assay, spheroid cultures were enzymatically dissociated in Accumax Reagent (Sigma-Aldrich), cell density was determined, and single cell suspensions were dispensed into 96-well black microplates with clear, flat bottom. Initial densities of 2000−3000 viable cells were chosen to be within the linear range of the assay at the chosen time point for all CSC lines. After plating, cells were incubated at 37 °C in 5% CO_2 for 24 h and then were treated with 1:3 serial dilutions of each compound (eight concentration points over a 0.023−50 μM concentration range), or with 0.1% DMSO as negative control. Three replicates for each experimental point were included. Cells were incubated at 37 °C in 5% CO_2 for 72 h, and then cell viability was determined using the CellTiter-Glo Luminescent Cell Viability Assay (Promega), essentially by following the manufacturer's recommendations. Compound cytotoxicity was evaluated in comparison to cells treated with DMSO. The CC_{50} values were determined by 4P logistic fitting of the experimental data with KaleidaGraph software based on the residual luminescence in the presence of increasing concentrations of the inhibitors.

For the EX-527/AGK-2 combination experiments, cells were treated in triplicate with 1:2 serial dilutions of each compound or with the combination of the two compounds (6.25−50 μM concentration range for CRC CSC 1.1 clone and 3.125−50 μM concentration range for GBM CSC 30P clone). Fractional response values were calculated relative to samples treated with DMSO, and dose−response curves for compounds EX-527 and AGK-2 administered individually or together were obtained by sigmoidal dose−response fitting of the experimental data using GraphPad Prism software. Bliss's independence (additivity) curves were derived by fitting the experimental data obtained with each individual compound into the Bliss's equation: $Y = FA + FB - (FA \times FB)$, where Y is the fractional response of the combination of the two drugs A and B assuming Bliss's independence.

■ ASSOCIATED CONTENT

Supporting Information

Chemical and physical data for compounds **2**−**6** and for the intermediate compounds **8a**, **8b**, **9a**−**c**, **10a**−**c**, **11a**−**c**, and **12b**. Modeling data and docking poses. Cell cycle and apoptosis induction at 5 and 50 μM in U937 cells. Antiproliferative activity in MOLT4 (at 25 and 100 μM), MDA-MB-231 (25 μM), and RKO (25 μM) cancer cells. Dose−response curves of the tested SIRT inhibitors in CSCs. This material is available free of charge via the Internet at http://pubs.acs.org.

■ AUTHOR INFORMATION

Corresponding Author

*Phone: +3906-4991-3392. Fax: +3906-491491. E-mail: antonello.mai@uniroma1.it.

Notes

The authors declare no competing financial interest.

■ ACKNOWLEDGMENTS

This work was supported by AIRC, PON01_01227, PRIN 2009PX2T2E, FIRB RBFR10ZJQT, and FP7 Project BLUEPRINT/282510.

■ ABBREVIATIONS USED

BCL-6, B-cell lymphoma 6; BDF4s, benzodeazaoxaflavins; bFGF, basic fibroblast growth factor; BOP reagent, benzotriazole-1-yl-oxy-tris-(dimethylamino)-phosphonium hexafluorophosphate reagent; CRC, colorectal carcinoma; CSCs, cancer stem cells; EGF, epidermal growth factor; FACS, fluorescence-activated cell sorting; FOXO1, forkhead box class O 1; GBM, glioblastoma multiforme; GDH, glutamate dehydrogenase; HeLa, Henrietta Lacks; HepG2, hepatocellular carcinoma G2; HOXA10, homeobox A10; MEF2, myocyte enhancer factor-2; MOE, molecular operating environment; MTT, (3-(4,5-dimethylthiazol-2-yl)-2,5-diphenyltetrazolium bromide; NF-kB, nuclear factor-kappa B; PGC1-α, peroxisome proliferator-activated receptor-γ coactivator 1-α; PI, propidium iodide

■ REFERENCES

(1) Arrowsmith, C. H.; Bountra, C.; Fish, P. V.; Lee, K.; Schapira, M. Epigenetic protein families: a new frontier for drug discovery. *Nature Rev. Drug Discovery* **2012**, *11*, 384−400.
(2) Jenuwein, T.; Allis, C. D. Translating the histone code. *Science* **2001**, *293*, 1074−1080.
(3) Jones, P. A.; Baylin, S. B. The epigenomics of cancer. *Cell* **2007**, *128*, 683−692.
(4) Yang, X. J.; Seto, E. HATs and HDACs: from structure, function and regulation to novel strategies for therapy and prevention. *Oncogene* **2007**, *26*, 5310−5318.
(5) Mai, A.; Massa, S.; Rotili, D.; Cerbara, I.; Valente, S.; Pezzi, R.; Simeoni, S.; Ragno, R. Histone deacetylation in epigenetics: an attractive target for anticancer therapy. *Med. Res. Rev.* **2005**, *25*, 261−309.
(6) Zheng, W. Mechanism-based modulator discovery for sirtuin-catalyzed deacetylation reaction. *Mini-Rev. Med. Chem.* **2012**, Jul 30, PMID 22876953.
(7) Cen, Y.; Youn, D. Y.; Sauve, A. A. Advances in characterization of human sirtuin isoforms: chemistries, targets and therapeutic applications. *Curr. Med. Chem.* **2011**, *18*, 1919−1935.
(8) Carafa, V.; Nebbioso, A.; Altucci, L. Sirtuins and disease: the road ahead. *Front. Pharmacol.* **2012**, *3*, 4.
(9) Haigis, M. C.; Sinclair, D. A. Mammalian sirtuins: biological insights and disease relevance. *Annu. Rev. Pathol.* **2010**, *5*, 253−295.
(10) Guarente, L.; Franklin, H. Epstein Lecture: Sirtuins, aging, and medicine. *N. Engl. J. Med.* **2011**, *364*, 2235−2244.
(11) Mostoslavsky, R.; Esteller, M.; Vaquero, A. At the crossroad of lifespan, calorie restriction, chromatin and disease: meeting on sirtuins. *Cell Cycle* **2010**, *9*, 1907−1912.
(12) Cen, Y. Sirtuins inhibitors: the approach to affinity and selectivity. *Biochim. Biophys. Acta* **2010**, *1804*, 1635−1644.
(13) Balcerczyk, A.; Pirola, L. Therapeutic potential of activators and inhibitors of sirtuins. *Biofactors* **2010**, *36*, 383−393.
(14) Stunkel, W.; Campbell, R. M. Sirtuin 1 (SIRT1): the misunderstood HDAC. *J. Biomol. Screening* **2011**, *16*, 1153−1169.
(15) Jung-Hynes, B.; Nihal, M.; Zhong, W.; Ahmad, N. Role of sirtuin histone deacetylase SIRT1 in prostate cancer. A target for prostate cancer management via its inhibition? *J. Biol. Chem.* **2009**, *284*, 3823−3832.
(16) Chen, J.; Zhang, B.; Wong, N.; Lo, A. W.; To, K. F.; Chan, A. W.; Ng, M. H.; Ho, C. Y.; Cheng, S. H.; Lai, P. B.; Yu, J.; Ng, H. K.; Ling, M. T.; Huang, A. L.; Cai, X. F.; Ko, B. C. Sirtuin 1 is upregulated in a subset of hepatocellular carcinomas where it is essential for telomere maintenance and tumor cell growth. *Cancer Res.* **2011**, *71*, 4138−4149.
(17) Jang, K. Y.; Kim, K. S.; Hwang, S. H.; Kwon, K. S.; Kim, K. R.; Park, H. S.; Park, B. H.; Chung, M. J.; Kang, M. J.; Lee, D. G.; Moon, W. S. Expression and prognostic significance of SIRT1 in ovarian epithelial tumours. *Pathology* **2009**, *41*, 366−371.
(18) Cha, E. J.; Noh, S. J.; Kwon, K. S.; Kim, C. Y.; Park, B. H.; Park, H. S.; Lee, H.; Chung, M. J.; Kang, M. J.; Lee, D. G.; Moon, W. S.; Jang, K. Y. Expression of DBC1 and SIRT1 is associated with poor prognosis of gastric carcinoma. *Clin. Cancer Res.* **2009**, *15*, 4453−4459.
(19) Nosho, K.; Shima, K.; Irahara, N.; Kure, S.; Firestein, R.; Baba, Y.; Toyoda, S.; Chen, L.; Hazra, A.; Giovannucci, E. L.; Fuchs, C. S.; Ogino, S. SIRT1 histone deacetylase expression is associated with microsatellite instability and CpG island methylator phenotype in colorectal cancer. *Mod. Pathol.* **2009**, *22*, 922−932.
(20) Kabra, N.; Li, Z.; Chen, L.; Li, B.; Zhang, X.; Wang, C.; Yeatman, T.; Coppola, D.; Chen, J. SirT1 is an inhibitor of

proliferation and tumor formation in colon cancer. *J. Biol. Chem.* **2009**, *284*, 18210−18217.
(21) Powell, M. J.; Casimiro, M. C.; Cordon-Cardo, C.; He, X.; Yeow, W. S.; Wang, C.; McCue, P. A.; McBurney, M. W.; Pestell, R. G. Disruption of a Sirt1-dependent autophagy checkpoint in the prostate results in prostatic intraepithelial neoplasia lesion formation. *Cancer Res.* **2011**, *71*, 964−975.
(22) Herranz, D.; Serrano, M. SIRT1: recent lessons from mouse models. *Nature Rev. Cancer* **2010**, *10*, 819−823.
(23) Nemoto, S.; Fergusson, M. M.; Finkel, T. Nutrient availability regulates SIRT1 through a forkhead-dependent pathway. *Science* **2004**, *306*, 2105−2108.
(24) Wang, R. H.; Sengupta, K.; Li, C.; Kim, H. S.; Cao, L.; Xiao, C.; Kim, S.; Xu, X.; Zheng, Y.; Chilton, B.; Jia, R.; Zheng, Z. M.; Appella, E.; Wang, X. W.; Ried, T.; Deng, C. X. Impaired DNA damage response, genome instability, and tumorigenesis in SIRT1 mutant mice. *Cancer Cell* **2008**, *14*, 312−323.
(25) Rajendran, R.; Garva, R.; Krstic-Demonacos, M.; Demonacos, C. Sirtuins: molecular traffic lights in the crossroad of oxidative stress, chromatin remodeling, and transcription. *J. Biomed. Biotechnol.* **2011**, *2011*, 368276.
(26) Firestein, R.; Blander, G.; Michan, S.; Oberdoerffer, P.; Ogino, S.; Campbell, J.; Bhimavarapu, A.; Luikenhuis, S.; de Cabo, R.; Fuchs, C.; Hahn, W. C.; Guarente, L. P.; Sinclair, D. A. The SIRT1 deacetylase suppresses intestinal tumorigenesis and colon cancer growth. *PLoS One* **2008**, *3*, e2020.
(27) Boily, G.; He, X. H.; Pearce, B.; Jardine, K.; McBurney, M. W. SirT1-null mice develop tumors at normal rates but are poorly protected by resveratrol. *Oncogene* **2009**, *28*, 2882−2893.
(28) Li, Y.; Matsumori, H.; Nakayama, Y.; Osaki, M.; Kojima, H.; Kurimasa, A.; Ito, H.; Mori, S.; Katoh, M.; Oshimura, M.; Inoue, T. SIRT2 down-regulation in HeLa can induce p53 accumulation via p38 MAPK activation-dependent p300 decrease, eventually leading to apoptosis. *Genes Cells* **2011**, *16*, 34−45.
(29) He, X.; Nie, H.; Hong, Y.; Sheng, C.; Xia, W.; Ying, W. SIRT2 activity is required for the survival of C6 glioma cells. *Biochem. Biophys. Res. Commun.* **2012**, *417*, 468−472.
(30) Zuo, Q.; Wu, W.; Li, X.; Zhao, L.; Chen, W. HDAC6 and SIRT2 promote bladder cancer cell migration and invasion by targeting cortactin. *Oncol. Rep.* **2012**, *27*, 819−824.
(31) Peck, B.; Chen, C. Y.; Ho, K. K.; Di Fruscia, P.; Myatt, S. S.; Coombes, R. C.; Fuchter, M. J.; Hsiao, C. D.; Lam, E. W. SIRT inhibitors induce cell death and p53 acetylation through targeting both SIRT1 and SIRT2. *Mol. Cancer Ther.* **2010**, *9*, 844−855.
(32) Bitterman, K. J.; Anderson, R. M.; Cohen, H. Y.; Latorre-Esteves, M.; Sinclair, D. A. Inhibition of silencing and accelerated aging by nicotinamide, a putative negative regulator of yeast sir2 and human SIRT1. *J. Biol. Chem.* **2002**, *277*, 45099−45107.
(33) Grozinger, C. M.; Chao, E. D.; Blackwell, H. E.; Moazed, D.; Schreiber, S. L. Identification of a class of small molecule inhibitors of the sirtuin family of NAD-dependent deacetylases by phenotypic screening. *J. Biol. Chem.* **2001**, *276*, 38837−38843.
(34) Heltweg, B.; Gatbonton, T.; Schuler, A. D.; Posakony, J.; Li, H.; Goehle, S.; Kollipara, R.; Depinho, R. A.; Gu, Y.; Simon, J. A.; Bedalov, A. Antitumor activity of a small-molecule inhibitor of human silent information regulator 2 enzymes. *Cancer Res.* **2006**, *66*, 4368−4377.
(35) Kalle, A. M.; Mallika, A.; Badiger, J.; Alinakhi; Talukdar, P.; Sachchidanand.. Inhibition of SIRT1 by a small molecule induces apoptosis in breast cancer cells. *Biochem. Biophys. Res. Commun.* **2010**, *401*, 13−19.
(36) Rotili, D.; Tarantino, D.; Carafa, V.; Lara, E.; Meade, S.; Botta, G.; Nebbioso, A.; Schemies, J.; Jung, M.; Kazantsev, A. G.; Esteller, M.; Fraga, M. F.; Altucci, L.; Mai, A. Identification of tri- and tetracyclic pyrimidinediones as sirtuin inhibitors. *ChemMedChem* **2010**, *5*, 674−677.
(37) Lain, S.; Hollick, J. J.; Campbell, J.; Staples, O. D.; Higgins, M.; Aoubala, M.; McCarthy, A.; Appleyard, V.; Murray, K. E.; Baker, L.; Thompson, A.; Mathers, J.; Holland, S. J.; Stark, M. J.; Pass, G.; Woods, J.; Lane, D. P.; Westwood, N. J. Discovery, in vivo activity, and mechanism of action of a small-molecule p53 activator. *Cancer Cell* **2008**, *13*, 454−463.
(38) Blum, C. A.; Ellis, J. L.; Loh, C.; Ng, P. Y.; Perni, R. B.; Stein, R. L. SIRT1 modulation as a novel approach to the treatment of diseases of aging. *J. Med. Chem.* **2011**, *54*, 417−432.
(39) Schemies, J.; Uciechowska, U.; Sippl, W.; Jung, M. NAD(+)-dependent histone deacetylases (sirtuins) as novel therapeutic targets. *Med. Res. Rev.* **2010**, *30*, 861−889.
(40) Villalba, J. M.; Alcain, F. J. Sirtuin activators and inhibitors. *Biofactors* **2012**, *38*, 349−359.
(41) Mai, A.; Massa, S.; Lavu, S.; Pezzi, R.; Simeoni, S.; Ragno, R.; Mariotti, F. R.; Chiani, F.; Camilloni, G.; Sinclair, D. A. Design, synthesis, and biological evaluation of sirtinol analogues as class III histone/protein deacetylase (Sirtuin) inhibitors. *J. Med. Chem.* **2005**, *48*, 7789−7795.
(42) Mai, A.; Valente, S.; Meade, S.; Carafa, V.; Tardugno, M.; Nebbioso, A.; Galmozzi, A.; Mitro, N.; De Fabiani, E.; Altucci, L.; Kazantsev, A. Study of 1,4-dihydropyridine structural scaffold: discovery of novel sirtuin activators and inhibitors. *J. Med. Chem.* **2009**, *52*, 5496−5504.
(43) Pasco, M. Y.; Rotili, D.; Altucci, L.; Farina, F.; Rouleau, G. A.; Mai, A.; Neri, C. Characterization of sirtuin inhibitors in nematodes expressing a muscular dystrophy protein reveals muscle cell and behavioral protection by specific sirtinol analogues. *J. Med. Chem.* **2010**, *53*, 1407−1411.
(44) Rotili, D.; Carafa, V.; Tarantino, D.; Botta, G.; Nebbioso, A.; Altucci, L.; Mai, A. Simplification of the tetracyclic SIRT1-selective inhibitor MC2141: coumarin- and pyrimidine-based SIRT1/2 inhibitors with different selectivity profile. *Bioorg. Med. Chem.* **2011**, *19*, 3659−3668.
(45) Orecchia, A.; Scarponi, C.; Di Felice, F.; Cesarini, E.; Avitabile, S.; Mai, A.; Mauro, M. L.; Sirri, V.; Zambruno, G.; Albanesi, C.; Camilloni, G.; Failla, C. M. Sirtinol treatment reduces inflammation in human dermal microvascular endothelial cells. *PLoS One* **2011**, *6*, e24307.
(46) Lara, E.; Mai, A.; Calvanese, V.; Altucci, L.; Lopez-Nieva, P.; Martinez-Chantar, M. L.; Varela-Rey, M.; Rotili, D.; Nebbioso, A.; Ropero, S.; Montoya, G.; Oyarzabal, J.; Velasco, S.; Serrano, M.; Witt, M.; Villar-Garea, A.; Imhof, A.; Mato, J. M.; Esteller, M.; Fraga, M. F. Salermide, a Sirtuin inhibitor with a strong cancer-specific proapoptotic effect. *Oncogene* **2009**, *28*, 781−791.
(47) Nguyen, L. V.; Vanner, R.; Dirks, P.; Eaves, C. J. Cancer stem cells: an evolving concept. *Nature Rev. Cancer* **2012**, *12*, 133−143.
(48) Prud'homme, G. J. Cancer stem cells and novel targets for antitumor strategies. *Curr. Pharm. Des.* **2012**, *18*, 2838−2849.
(49) Kubota, T.; Sawada, N.; Zhou, L.; Welch, C. J. Enantioseparation of benzazoles and benzanilides on polysaccharide-based chiral columns. *Chirality* **2010**, *22*, 382−388.
(50) Charton, J.; Girault-Mizzi, S.; Debreu-Fontaine, M. A.; Foufelle, F.; Hainault, I.; Bizot-Espiard, J. G.; Caignard, D. H.; Sergheraert, C. Synthesis and biological evaluation of benzimidazole derivatives as potent AMP-activated protein kinase activators. *Bioorg. Med. Chem.* **2006**, *14*, 4490−4518.
(51) Yang, Q.; Olmsted, C.; Borhan, B. Absolute stereochemical determination of chiral carboxylic acids. *Org. Lett.* **2002**, *4*, 3423−3426.
(52) Bissinger, E. M.; Heinke, R.; Spannhoff, A.; Eberlin, A.; Metzger, E.; Cura, V.; Hassenboehler, P.; Cavarelli, J.; Schule, R.; Bedford, M. T.; Sippl, W.; Jung, M. Acyl derivatives of *p*-aminosulfonamides and dapsone as new inhibitors of the arginine methyltransferase hPRMT1. *Bioorg. Med. Chem.* **2011**, *19*, 3717−3731.
(53) Napper, A. D.; Hixon, J.; McDonagh, T.; Keavey, K.; Pons, J. F.; Barker, J.; Yau, W. T.; Amouzegh, P.; Flegg, A.; Hamelin, E.; Thomas, R. J.; Kates, M.; Jones, S.; Navia, M. A.; Saunders, J. O.; DiStefano, P. S.; Curtis, R. Discovery of indoles as potent and selective inhibitors of the deacetylase SIRT1. *J. Med. Chem.* **2005**, *48*, 8045−8054.
(54) Solomon, J. M.; Pasupuleti, R.; Xu, L.; McDonagh, T.; Curtis, R.; DiStefano, P. S.; Huber, L. J. Inhibition of SIRT1 catalytic activity

increases p53 acetylation but does not alter cell survival following DNA damage. *Mol. and cell. biol.* **2006**, *26*, 28−38.
(55) Outeiro, T. F.; Kontopoulos, E.; Altmann, S. M.; Kufareva, I.; Strathearn, K. E.; Amore, A. M.; Volk, C. B.; Maxwell, M. M.; Rochet, J. C.; McLean, P. J.; Young, A. B.; Abagyan, R.; Feany, M. B.; Hyman, B. T.; Kazantsev, A. G. Sirtuin 2 inhibitors rescue alpha-synuclein-mediated toxicity in models of Parkinson's disease. *Science* **2007**, *317*, 516−519.
(56) Wang, T. T.; Schoene, N. W.; Kim, E. K.; Kim, Y. S. Pleiotropic effects of the sirtuin inhibitor sirtinol involves concentration-dependent modulation of multiple nuclear receptor-mediated pathways in androgen-responsive prostate cancer cell LNCaP. *Mol. Carcinog.* **2012**, DOI 10.1002/mc.21906.
(57) Ricci-Vitiani, L.; Lombardi, D. G.; Pilozzi, E.; Biffoni, M.; Todaro, M.; Peschle, C.; De Maria, R. Identification and expansion of human colon-cancer-initiating cells. *Nature* **2007**, *445*, 111−115.
(58) Ricci-Vitiani, L.; Pallini, R.; Larocca, L. M.; Lombardi, D. G.; Signore, M.; Pierconti, F.; Petrucci, G.; Montano, N.; Maira, G.; De Maria, R. Mesenchymal differentiation of glioblastoma stem cells. *Cell Death Differ.* **2008**, *15*, 1491−1498.